Trans Indian Inst Met (2020) 73(9):2403–2413
https://doi.org/10.1007/s12666-020-02044-1

ORIGINAL ARTICLE

# Parameter Optimization in Incremental Forming of Titanium Alloy Material

**C. Veera ajay**[1]

Received: 30 January 2020 / Accepted: 14 July 2020 / Published online: 30 July 2020


**Abstract** Incremental forming is a flexible and adaptable process with a high scope in future for prototyping sector and batch shop production. It finds application in almost every engineering field. One such prominent field is the research and development. The research and development are often associated with prototyping of a variety of products for evaluating and testing the design and clarifying production costs and issues. In this paper, experimentation of Ti-6Al-4V sheets using SPIF was studied, and the influence of tool feed (*f*), incremental step depth (*d*) and spindle speed (*s*) to the surface roughness ($R_a$), wall angle ($\theta$), and average thickness (*t*) were evaluated. The method was carried out using CNC Milling Machine with the help of a fixture and hemispherical end tool. Response surface methodology was used to design the experiments, and ANOVA was performed to find the factor which affected the selected method significantly. Finally, the input parameters were optimized to achieve maximum wall thickness, minimum surface roughness, and maximum wall angle.

**Keywords** Sheet metal · CNC machine tool · CAD/CAM · Response surface methodology · ANOVA

✉ C. Veera ajay
ajayveera2@gmail.com

[1] Department of Mechanical Engineering, National Engineering College, Kovilpatti, India

## 1 Introduction

Incremental sheet forming (ISF) is a dieless sheet forming process which can reduce the high tooling cost associated with the traditional process and increase the customizability making it suitable for prototyping and in low volume production industries like aerospace, automotive, biomedical, etc. [1]. The incremental sheet forming process has better formability than other conventional sheet metal forming techniques due to localized deformations in ISF. Kopac and Kampus [2] used the ball-type forming tool with 10 mm diameter and used grease as lubricant which improved tribological characteristics. Park et al. [3] have compared the traditional sheet forming with the incremental sheet forming and have found that forming limit curve appears in a different pattern in ISF. The low step depth has increased the formability limit. Cerro et al. [4] used finite element analyses to predict accurately the response parameters such as geometrical accuracy, sheet thickness, and roughness of formed component. The FEA was carried out using ABAQUS explicit software, and results have been compared to the actual experimentation. The low incremental depth and application of lubricant between the contact surfaces have significantly improved the surface finish. Araghi et al. [5] combined the stretch forming process and incremental sheet metal forming process. The combined process has been observed to be similar to the two-point incremental forming. Sheet thinning in SPIF and combined process have been compared and studied in detail. Finite element simulation procedure has been set up for pure incremental sheet forming and combined process. Uniform thickness distribution and reduction in forming time have been found in the combined process. Results of Minutolo et al. [6] indicate that higher wall angles can be formed in cone shapes when compared

**Fig. 1** Experimental setup in LV 45—CNC Vertical Machining Centre

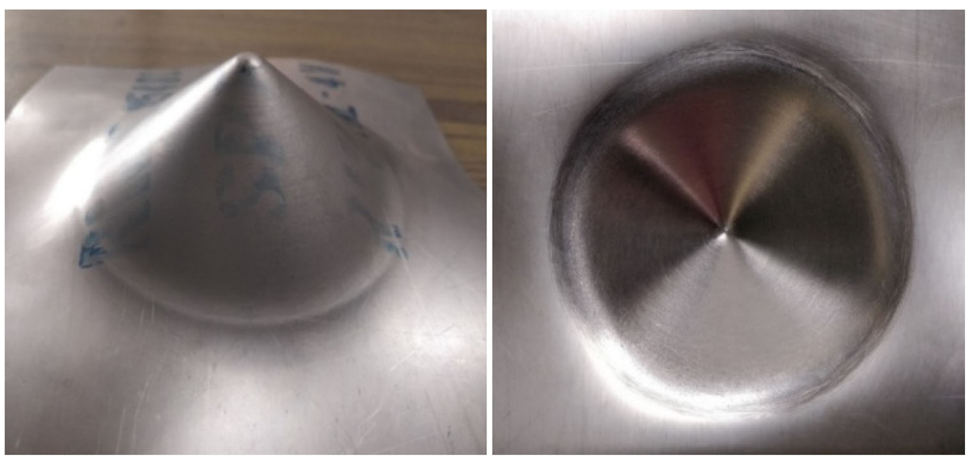
**Fig. 2** Incrementally formed sheet metal

to pyramid shapes. Numerical simulations performed using LS-DYNA reveals that it is possible to form free surfaces relevant to different strain conditions including the most stressed zone that acts as the fracture points. Yao et al. [7] optimized the input parameters such as tool diameter, step depth, and sheet thickness over response parameters such as deformation energy, geometric error, and surface roughness. Experiments have been carried out in Al1060 sheets using a hemispherical end tool made of X210CrW12. The process variables relation has been studied using response surface methodology and a regression model has been developed. It is found that increasing the tool diameter has increased the deformation energy but decreased the accuracy and surface roughness. Jadhav [8] used the helical tool path for incrementally forming the sheet metal which results in twist and dents in the final formed components. To overcome this defects, the sheet is formed using either the tool path with distributed increment or bi-directional tool path and also has improved the geometric accuracy of the part. This selected tool path has distributed the forces uniformly along the edge of the geometry which has been the factor for increasing geometric accuracy. Reddy et al. [9] analyzed the formability and surface finish of Al 5052 alloy by incrementally forming the truncated cones and truncated pyramids using Box–Behnken method. It has been reported that for all

**Table 1** Input parameters and output response values

| Run | Spindle speed (rpm) | Tool feed (mm/min) | Incremental step depth (mm) | Formed wall thickness (mm) | Wall angle (degree) | Surface roughness (microns) |
|---|---|---|---|---|---|---|
| 1 | 100 | 2000 | 0.3 | 0.38 | 27.16 | 1.04 |
| 2 | 200 | 2000 | 0.3 | 0.36 | 27.52 | 1.08 |
| 3 | 150 | 1500 | 0.2 | 0.42 | 28.43 | 0.94 |
| 4 | 150 | 2000 | 0.2 | 0.38 | 28.38 | 0.85 |
| 5 | 150 | 1500 | 0.2 | 0.38 | 28.65 | 0.92 |
| 6 | 200 | 2000 | 0.1 | 0.42 | 29.63 | 0.72 |
| 7 | 200 | 1000 | 0.3 | 0.38 | 27.92 | 1.19 |
| 8 | 150 | 1500 | 0.3 | 0.36 | 27.67 | 1.1 |
| 9 | 100 | 1000 | 0.3 | 0.4 | 27.45 | 1.14 |
| 10 | 200 | 1000 | 0.1 | 0.44 | 29.74 | 0.83 |
| 11 | 100 | 1500 | 0.2 | 0.38 | 28.20 | 0.88 |
| 12 | 150 | 1500 | 0.2 | 0.38 | 28.45 | 0.92 |
| 13 | 100 | 1000 | 0.1 | 0.46 | 29.39 | 0.8 |
| 14 | 150 | 1500 | 0.2 | 0.4 | 28.32 | 0.96 |
| 15 | 150 | 1000 | 0.2 | 0.4 | 28.85 | 1.02 |
| 16 | 200 | 1500 | 0.2 | 0.38 | 28.88 | 0.98 |
| 17 | 150 | 1500 | 0.2 | 0.38 | 28.78 | 0.92 |
| 18 | 150 | 1500 | 0.1 | 0.44 | 29.61 | 0.77 |
| 19 | 150 | 1500 | 0.2 | 0.4 | 28.70 | 0.9 |
| 20 | 100 | 2000 | 0.1 | 0.42 | 29.10 | 0.74 |

**Table 2** ANOVA table for surface roughness

| Source | Sum of squares | Df | Mean square | *F* value | *P* value Prob > *F* | |
|---|---|---|---|---|---|---|
| Model | 0.32 | 9 | 0.036 | 52.03 | < 0.0001 | Significant |
| *L*-spindle speed | 4.000E−003 | 1 | 4.000E−003 | 5.81 | 0.0366 | Significant |
| *M*-incremental step depth | 0.29 | 1 | 0.29 | 415.08 | < 0.0001 | Significant |
| *N*-tool feed | 0.030 | 1 | 0.030 | 43.96 | < 0.0001 | Significant |
| LM | 8.000E−004 | 1 | 8.000E−004 | 1.16 | 0.3062 | |
| LN | 4.500E−004 | 1 | 4.500E−004 | 0.65 | 0.4375 | |
| MN | 2.000E−004 | 1 | 2.000E−004 | 0.29 | 0.6016 | |
| *L*^2 | 9.091E−006 | 1 | 9.091E−006 | 0.013 | 0.9108 | |
| *M*^2 | 1.278E−004 | 1 | 1.278E−004 | 0.19 | 0.6756 | |
| *N*^2 | 1.278E−004 | 1 | 1.278E−004 | 0.19 | 0.6756 | |
| Residual | 6.881E−003 | 10 | 6.881E−004 | | | |
| Lack of fit | 4.748E−003 | 5 | 9.495E−004 | 2.23 | 0.2003 | Not significant |
| Pure error | 2.133E−003 | 5 | 4.267E−004 | | | |
| Cor total | 0.33 | 19 | | | | |
| SD = 0.026 | | Mean = 0.93 | | | | PRESS = 0.043 |
| *R*-Squared = 0.9791 | | Adj *R*-Squared = 0.9603 | | | | Pred *R*-Squared = 0.8703 |

incremental depths, surface roughness decreases with increases in tool diameter. Surface roughness up to certain angle increases with increase in incremental depth and then decreases. The surface roughness value decreases as the wall angle increases. Hussaina et al. [10] have found that Al-1060-H24 (hardening exponent = 0.042) provides 7.5% higher formability than Stainless Steel 304A (hardening exponent = 0.53). Hence, it has been concluded that less hardening exponent produces high formability of the sheet metal.

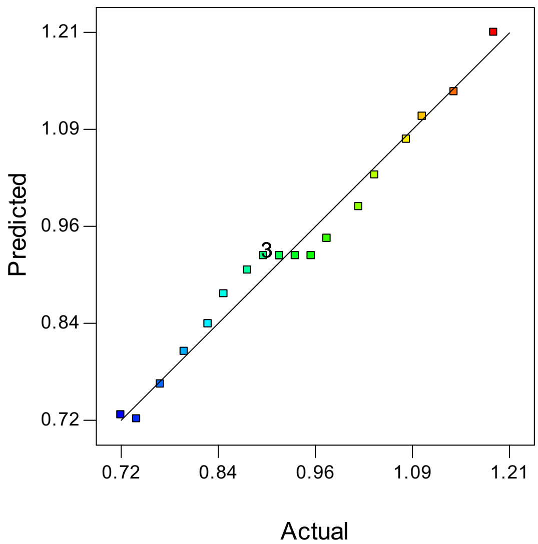


**Fig. 3** Predicted response versus actual response for surface roughness

## 2 Materials and Methods

The Ti-6Al-4V alloy material of thickness 0.6 mm and 16 mm hemispherical tool were selected for the optimization. The experiments were conducted using a 3-Axis CNC milling machine (LMW LV45) which is shown in Fig. 1. A specialized fixture setup was designed and manufactured for the sole purpose of incrementally forming the 150 × 150 mm sheets. The formed cone specimen is shown in Fig. 2. The design of experiment's layout containing the input process parameters and the output responses are given in Table 1.

## 3 Results and Discussion

The experiment based on central composite design (CCD) is conducted, and the obtained responses are analyzed for optimal conditions for the surface roughness, wall angle, and thinning. ANOVA is performed for the design of experiment to obtain the factors that significantly affect the single point incremental sheet forming (SPIF) of Ti-6Al-4V alloy material.

### 3.1 Surface Roughness

Table 2 shows the ANOVA for surface roughness at 95% confidence interval (α = 95%), respectively. The *P* value in the range of 0–0.05 indicates that the factors are statistically significant in affecting the process and *P* value in the range of 0.05 to 0.1 indicates that factors are marginally significant, whereas factors whose *P* value is above 0.1 indicate their insignificance in affecting the process. Significant model terms are *L*, *M*, *N*. The obtained value of $R^2$ is 0.9791 for surface roughness which indicates that the model is 97.91% capable to predict the response value. The $R^2$ value is in good agreement with the adjusted $R^2$ (0.9603), and the "Pred *R*-Squared" of 0.8703 is in reasonable agreement with the "Adj *R*-Squared" of 0.9603. Therefore, this model can be used to predict the surface roughness within the selected parameter ranges. PRESS (stands for "Prediction Residual Sum of Squares") is a measure of how well a selected model fits every point in a design. The model is desirable if PRESS value is less, and hence, the obtained value of 0.043 makes the model desirable.

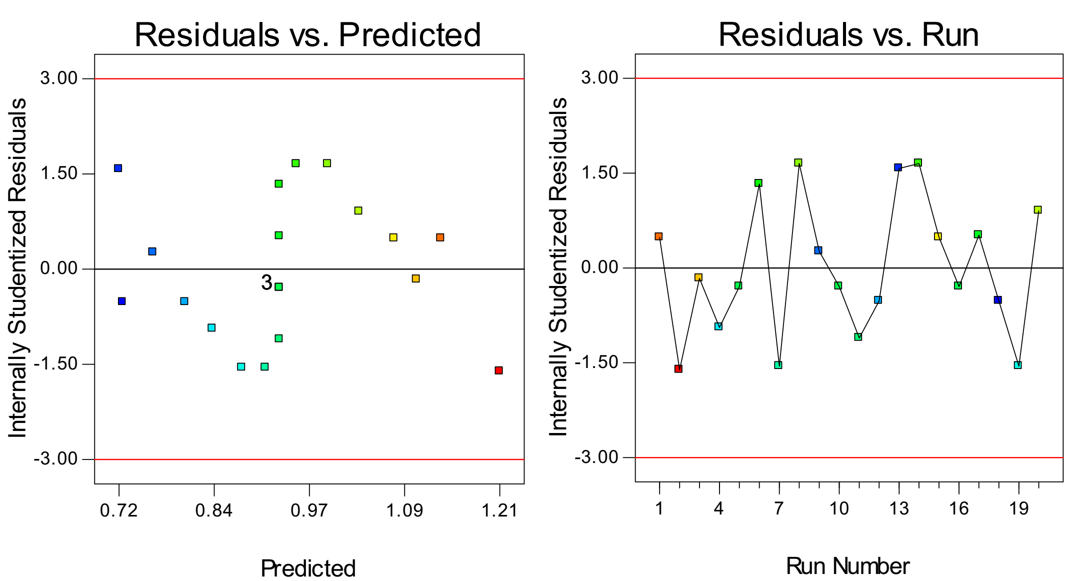


**Fig. 4** Residuals versus predicted and run number for surface roughness

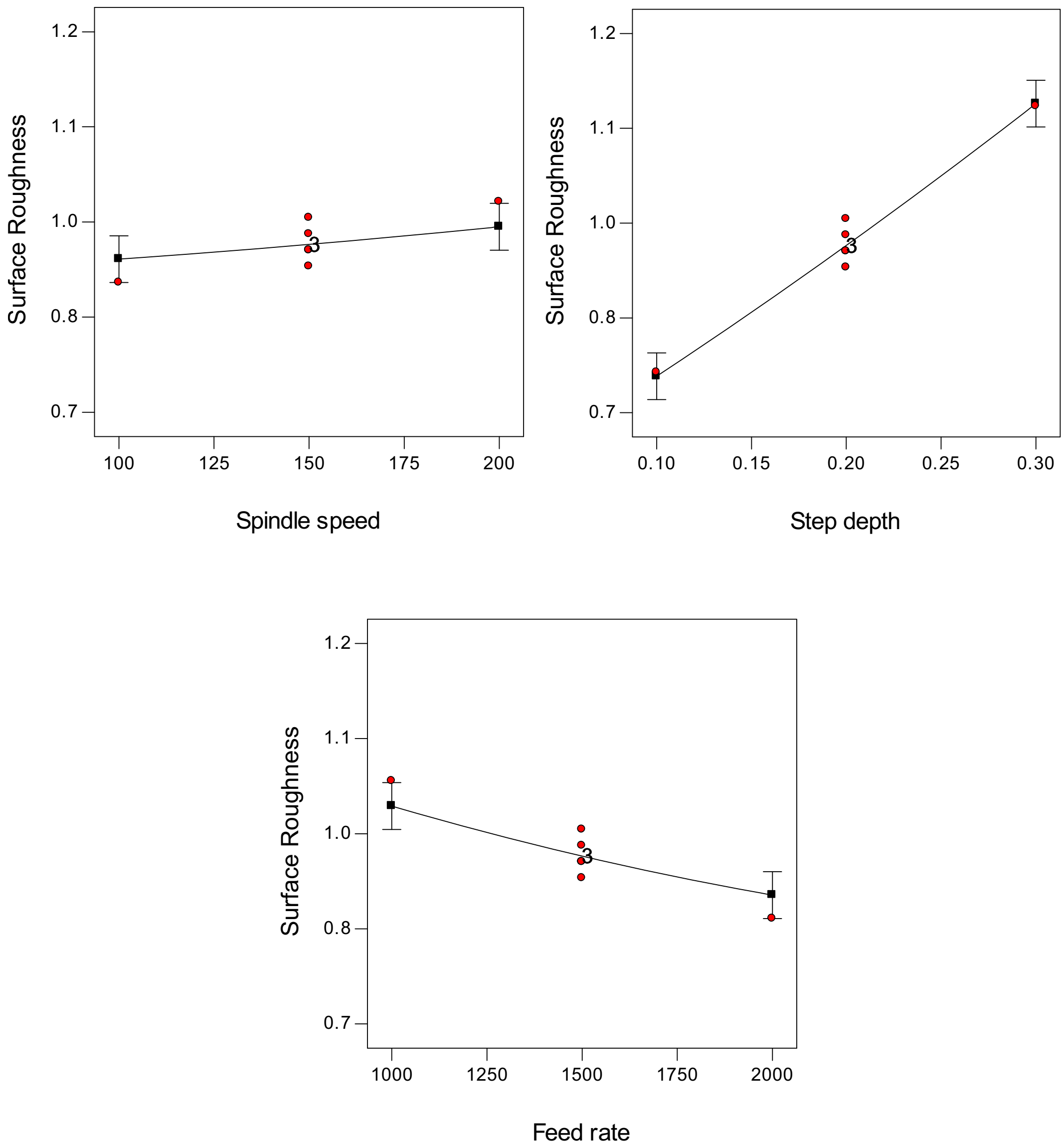


**Fig. 5** One-factor graph for surface roughness

The quadratic equation which fits the experimental model is given in the equation in terms of coded factors. The quadratic equation for $R_a$ is given in Eq. 1.

$$\begin{aligned}&\text{Surface Roughness } R_a\\&= 0.93 + 0.020 * L + 0.17 * M - 0.055 * N\\&+ 0.010 * L * M - 0.0075 * L * N - 0.005 * M * N\\&+ 0.00182 * L^2 + 0.00682 * M^2 + 0.00682 * N^2\end{aligned} \tag{1}$$

. Figure 3 shows the graph for surface roughness plotted against experimental and predicted values. Figure 4 shows the graph plotted for residuals versus predicted and run number for surface roughness.

One-factor analysis explains how individual factors affect the surface roughness upon changing their levels. From Fig. 5, the following information can be found: (1) With the increase in spindle speed from 100 to 200 rpm, there is only a small change in surface roughness from 0.9 µm to 1 µm. This indicates that friction does not play a major role in increasing the formability of this material. (2) With the increases in step depth from 0.1 mm to 0.3 mm, the surface roughness increases from 0.75 µm to 1.15 µm. The better surface finish is achieved when decreasing the step depth from 0.3 mm to 0.1 mm. (3) With the increases in feed rate from 1000 mm/min to 2000 mm/min, the surface roughness decreases from 1.05 µm to 0.9 µm.

**Table 3** ANOVA table for wall angle

| Source | Sum of squares | Df | Mean square | F value | $P$ value Prob > $F$ | |
|---|---|---|---|---|---|---|
| Model | 10.37 | 9 | 1.15 | 49.87 | < 0.0001 | Significant |
| $L$-spindle speed | 0.57 | 1 | 0.57 | 24.72 | 0.0006 | Significant |
| $M$-incremental step depth | 9.51 | 1 | 9.51 | 411.46 | < 0.0001 | Significant |
| $N$-tool feed | 0.24 | 1 | 0.24 | 10.53 | 0.0088 | Significant |
| LM | 3.125E−004 | 1 | 3.125E−004 | 0.014 | 0.9097 | |
| LN | 6.125E−004 | 1 | 6.125E−004 | 0.027 | 0.8739 | |
| MN | 0.011 | 1 | 0.011 | 0.46 | 0.5153 | |
| $L$^2 | 0.021 | 1 | 0.021 | 0.89 | 0.3683 | |
| $M$^2 | 5.114E−004 | 1 | 5.114E−004 | 0.022 | 0.8847 | |
| $N$^2 | 3.551E−004 | 1 | 3.551E−004 | 0.015 | 0.9038 | |
| Residual | 0.23 | 10 | 0.023 | | | |
| Lack of fit | 0.068 | 5 | 0.014 | 0.42 | 0.8177 | Not significant |
| Pure error | 0.16 | 5 | 0.033 | | | |
| Cor total | 10.60 | 19 | | | | |
| SD = 0.15 | | Mean = 28.54 | | | PRESS = 0.84 | |
| $R$-Squared = 0.9782 | | Adj $R$-Squared = 0.9586 | | | Pred $R$-Squared = 0.9203 | |

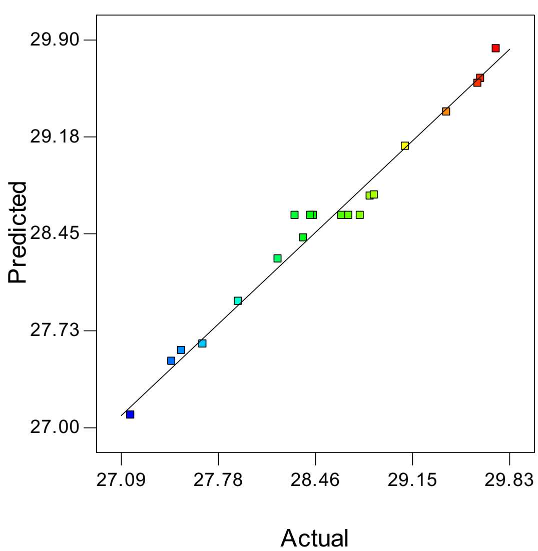


**Fig. 6** Predicted response versus actual response for wall angle

## 3.2 Wall Angle

Table 3 shows the ANOVA for wall angle at 95% confidence interval (α = 95%), respectively. Significant model terms are $L$, $M$, $N$. The obtained value of $R^2$ is 0.9782 for wall angle which indicates that the model is 97.82% capable to predict the response value. The $R^2$ value is in good agreement with the adjusted $R^2$ (0.9586), and the "Pred $R$-Squared" of 0.9203 is in reasonable concurrence with the "Adj $R$-Squared" of 0.9586. Therefore, this model can be used to predict the wall angle within the selected parameter ranges. The obtained PRESS value is lesser which makes the model desirable. Figure 6 shows the graph for wall angle plotted against experimental and predicted values. Figure 7 shows the graph plotted for residuals versus predicted and run number for wall angle.

The quadratic equation which fits the experimental model is given in the equation in terms of coded factors.

$$\text{Wall angle} = 28.53 + 0.24 * L - 0.97 * M - 0.16 * N - 0.00625 * L * M + 0.00875 * L * N - 0.036 * M * N - 0.086 * L^2 + 0.014 * M^2 - 0.011 * N^2 \quad (2)$$

One-factor analysis explains how individual factors affect the wall angle upon changing their levels. From Fig. 8, the following information can be found: (1) The spindle speed at 100 rpm has produced 28° wall angle and at 200 rpm has produced 28.7° wall angle which indicates that increase in spindle speed does not produce high variation in wall angle. (2) With the increase in step depth, the wall angle decreases greatly from 29.5° to 27.6° when using 0.1 mm and 0.3 mm step depth, respectively. (3) The feed rate also has not produced significant variations in wall angle as feed rate is associated with crossfeed and infeed.

## 3.3 Thinning (Measured Thickness)

Table 4 shows the ANOVA for thinning at 95% confidence interval (α = 95%), respectively. Here, $M$, $N$ are significant

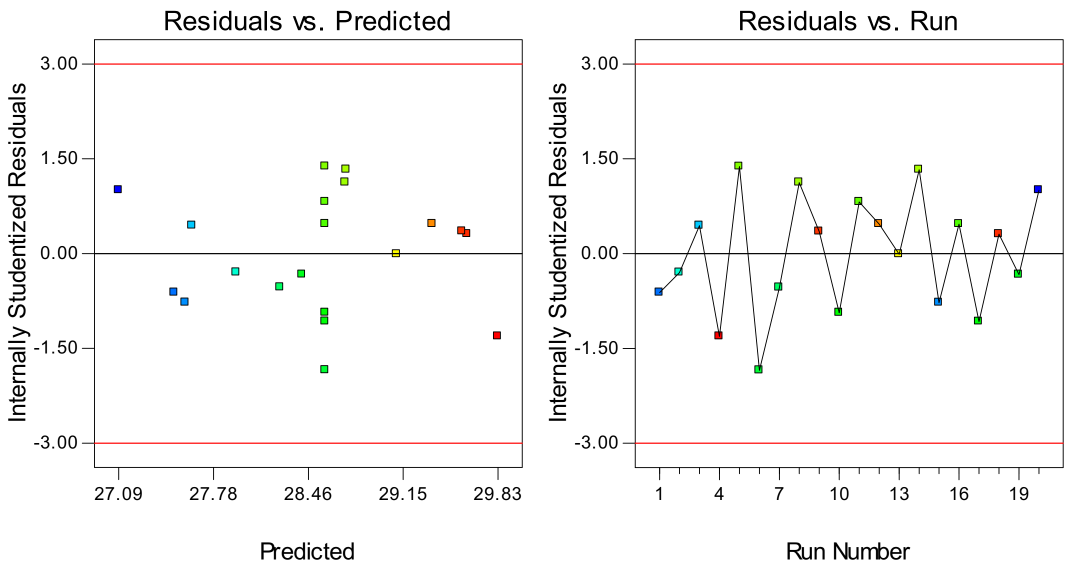


**Fig. 7** Residuals versus predicted and run number for Wall angle

**Fig. 8** One-factor graph for wall angle

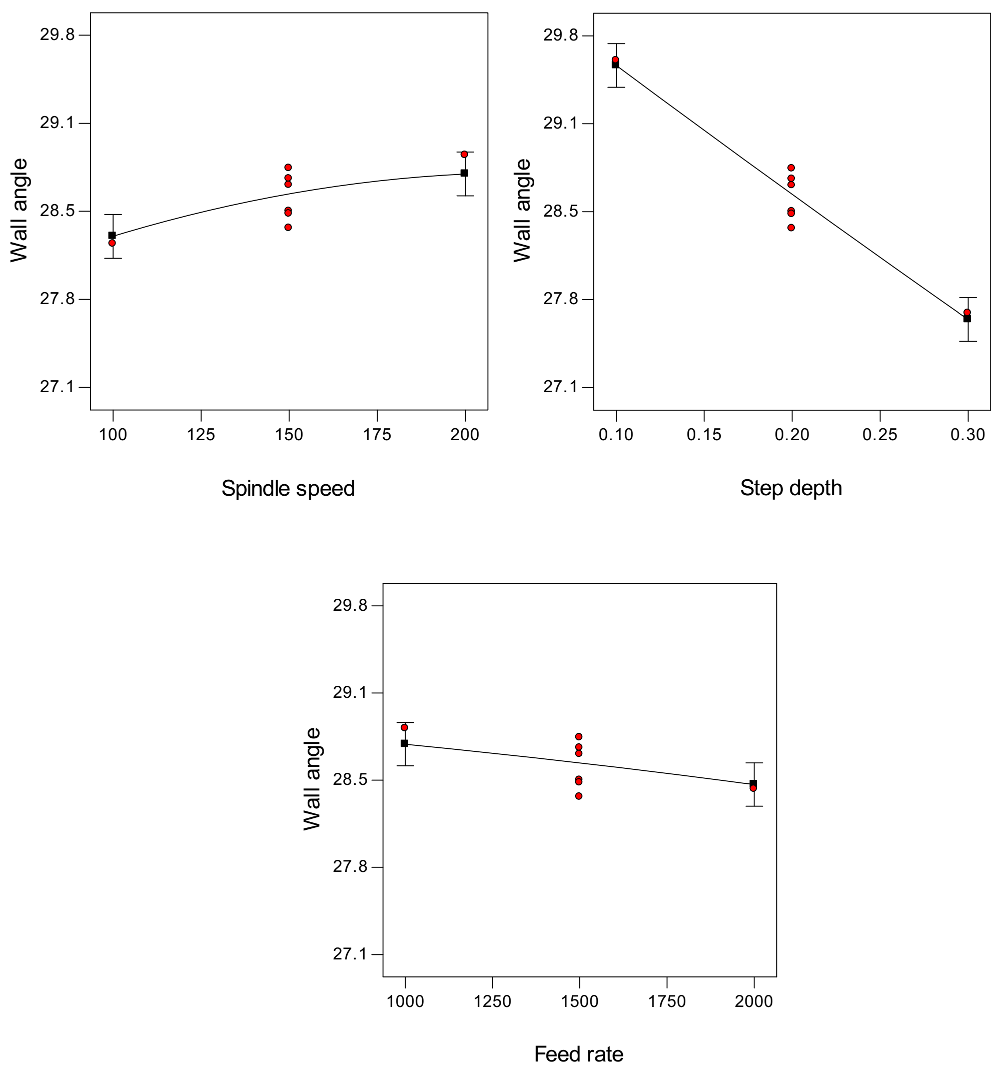

**Table 4** ANOVA table for thinning

| Source | Sum of squares | df | Mean square | F value | *P* value Prob > F | |
|---|---|---|---|---|---|---|
| Model | 0.012 | 9 | 1.370E−003 | 6.89 | 0.0029 | Significant |
| *L*-spindle speed | 3.600E−004 | 1 | 3.600E−004 | 1.81 | 0.2081 | Not significant |
| *M*-incremental step depth | 9.000E−003 | 1 | 9.000E−003 | 45.27 | < 0.0001 | Significant |
| *N*-tool feed | 1.440E−003 | 1 | 1.440E−003 | 7.24 | 0.0227 | Significant |
| LM | 5.000E−005 | 1 | 5.000E−005 | 0.25 | 0.6269 | |
| LN | 5.000E−005 | 1 | 5.000E−005 | 0.25 | 0.6269 | |
| MN | 5.000E−005 | 1 | 5.000E−005 | 0.25 | 0.6269 | |
| *L*^2 | 5.682E−005 | 1 | 5.682E−005 | 0.29 | 0.6046 | |
| *M*^2 | 6.568E−004 | 1 | 6.568E−004 | 3.30 | 0.0992 | Marginally significant |
| *N*^2 | 8.182E−005 | 1 | 8.182E−005 | 0.41 | 0.5356 | |
| Residual | 1.988E−003 | 10 | 1.988E−004 | | | |
| Lack of fit | 6.548E−004 | 5 | 1.310E−004 | 0.49 | 0.7731 | Not significant |
| Pure error | 1.333E−003 | 5 | 2.667E−004 | | | |
| Cor total | 0.014 | 19 | | | | |
| SD = 0.014 | | | Mean = 0.40 | | | PRESS = 0.006664 |
| *R*-Squared = 0.8612 | | | Adj *R*-Squared = 0.7362 | | | Pred *R*-Squared = 0.5346 |

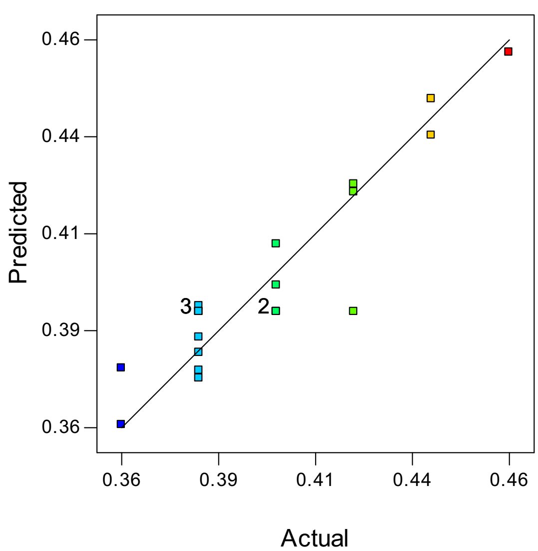


**Fig. 9** Predicted response versus actual response for thinning

model terms and $M^2$ is marginally significant model term. The obtained value of $R^2$ is 0.8612 for thinning which indicates that the model is 86.12% capable to predict the response value. The $R^2$ value is in reasonable concurrence with the adjusted $R^2$ (0.7362). Therefore, this model can be used to predict the thinning within the selected parameter ranges. The lesser value of PRESS is desirable, and hence, the obtained PRESS value is 0.006664 which makes the model desirable.

The quadratic equation which fits the experimental model is given in the equation in terms of coded factors.

$$\begin{aligned}\text{Thinning} &= 0.39 - 0.006 * L - 0.030 * M \\ &\quad - 0.012 * N - 0.0025 * L * M \\ &\quad + 0.0025 * L * N + 0.0025 * M * N \\ &\quad - 0.004545 * L^2 + 0.015 * M^2 + 0.005455 * N^2\end{aligned} \quad (3)$$

. Figure 9 shows the graph for thinning plotted against experimental and predicted values. Figure 10 shows the graph plotted for residuals versus predicted and run number for thinning.

One-factor analysis explains how individual factors affect the average thickness of the formed sheet metal upon changing their levels. From Fig. 11, the following information can be found: (1) As the spindle speed increases from 100 to 200 rpm, the thickness of the sheet decreases slightly from 0.395 mm to 0.385 mm which shows that increase in spindle speed does not produce high variation in thinning of the sheet metal. (2) With the increase in step depth, the thickness of the formed sheet metal decreases greatly from 0.43 mm to 0.38 mm when using 0.1 mm and 0.3 mm step depth, respectively. (3) The feed rate also produces only significant amount of variations in thinning of sheet metal.

### 3.4 Desirability-Based Optimization

In the RSM, desirability-based optimization has been performed for the multiresponse optimization. The desirability *d* = 0 denotes that the response is completely intolerable, whereas *d* = 1 denotes that the response is closely of the target value. Table 5 shows the upper limits, the lower

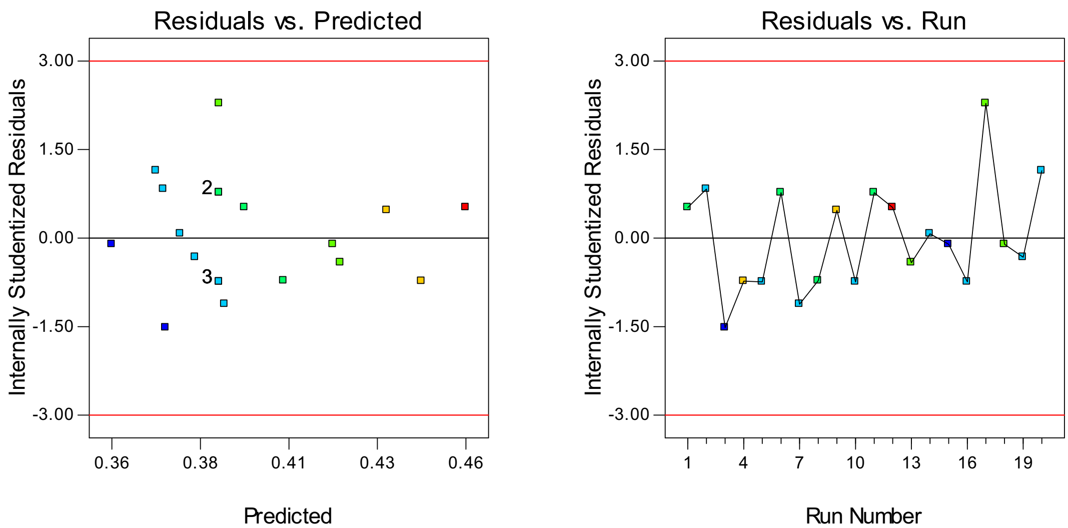


**Fig. 10** Residuals versus predicted and run number for thinning

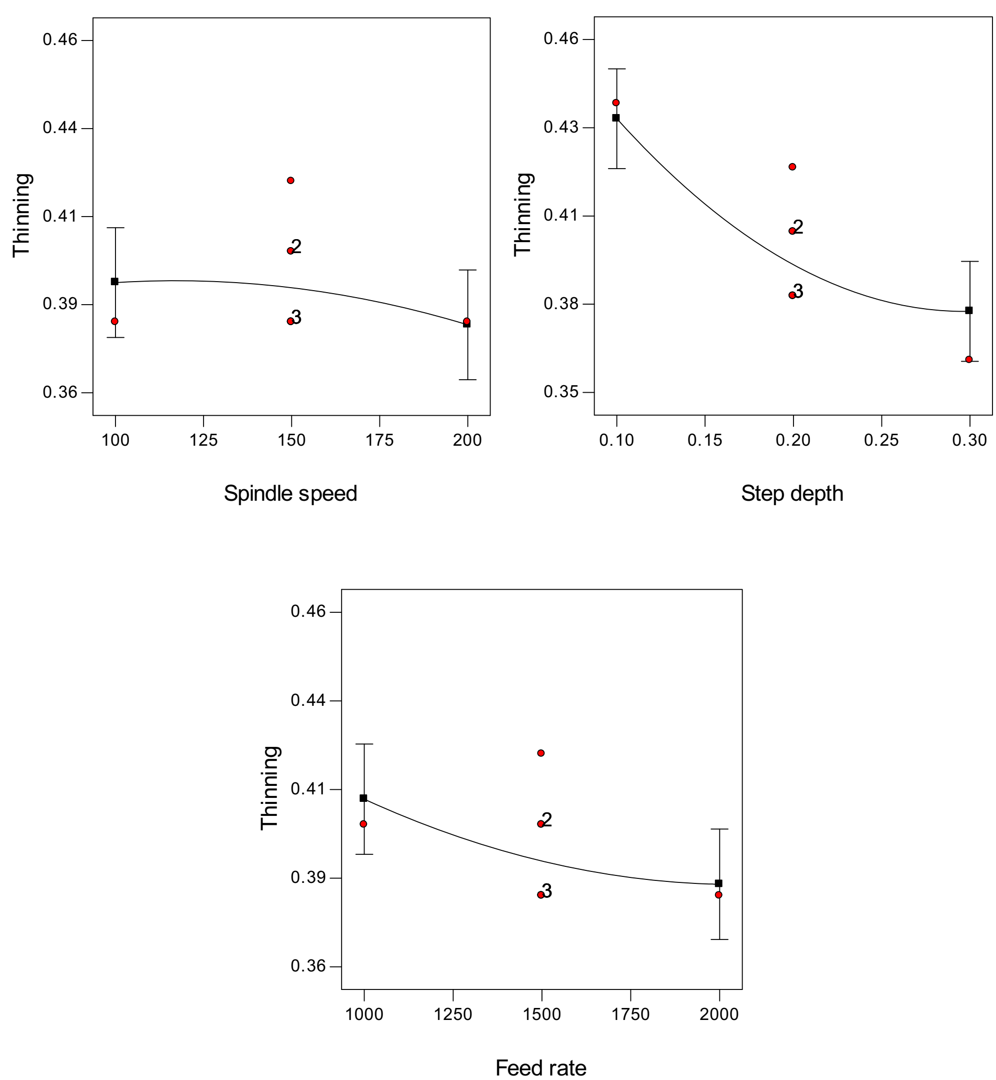


**Fig. 11** One-factor graph for thinning

**Table 5** Goals set and limits used for optimization

| Constraints name | Goal | Lower limit | Upper limit |
|---|---|---|---|
| Spindle speed | Is in range | 100 | 200 |
| Incremental step depth | Is in range | 0.1 | 0.3 |
| Tool feed | Is in range | 1000 | 2000 |
| Surface roughness | Minimize | 0.72 | 1.19 |
| Wall angle | Maximize | 27.16 | 29.74 |
| Thinning | Maximize | 0.36 | 0.46 |

limits, goals set used for optimization. The highest desirability solution is selected as optimal value, and the same is shown in Table 6. The histogram of the desirability of the best solution is shown in Fig. 12.

Numerical optimization is an algorithm which is similar to hill climbing technique. The desirability is a measure of how possibly the optimized response can be obtained. The desirability should always be closer to 1. Considering output responses such as surface roughness, thinning, and wall angle, the best optimized combination of values is 0.8 µm, 0.46 mm, and 29.7° which can be obtained when formed with 150 rpm spindle speed, 0.1 mm step depth, and 1000 mm/min tool feed which is shown in Fig. 13. The desirability to obtain the same responses when run using the optimized process parameters is 90%.

### 3.5 Confirmatory Experiment

The confirmatory experiment was performed with the optimized process parameters obtained from the numerical optimization. The confirmatory experiment has produced component with surface roughness of 0.78 µm, thinning of 0.44 mm, and wall angle of 29.76° which has deviate by only 2.5%, 4.5%, and 0.2% respectively.

## 4 Conclusion

a. The obtained value of $R^2$ is 0.9791, 0.9782, 0.8612 for surface roughness, wall angle, thinning, respectively, which indicates that the model is 97.91%, 97.82%, 86.12% capable to predict the response value.
b. Incremental depth and tool feed are the significant parameters that affects the selected response parameters.
c. The best optimal global solutions are as follows

| | | |
|---|---|---|
| Spindle speed | Incremental step depth | Tool feed |
| 146.09 rpm | 0.10 mm | 1000.00 mm/mn |
| Surface roughness | Wall angle | Thinning |
| 0.82 µm | 29.7° | 0.46 mm |

**Table 6** Best global solutions for optimization

| Number | Spindle speed | Incremental step depth | Tool feed | Surface roughness | Wall angle | Thinning | Desirability |
|---|---|---|---|---|---|---|---|
| 1 | 146.09 | 0.10 | 1000.00 | 0.82 | 29.7 | 0.46 | 0.900 |

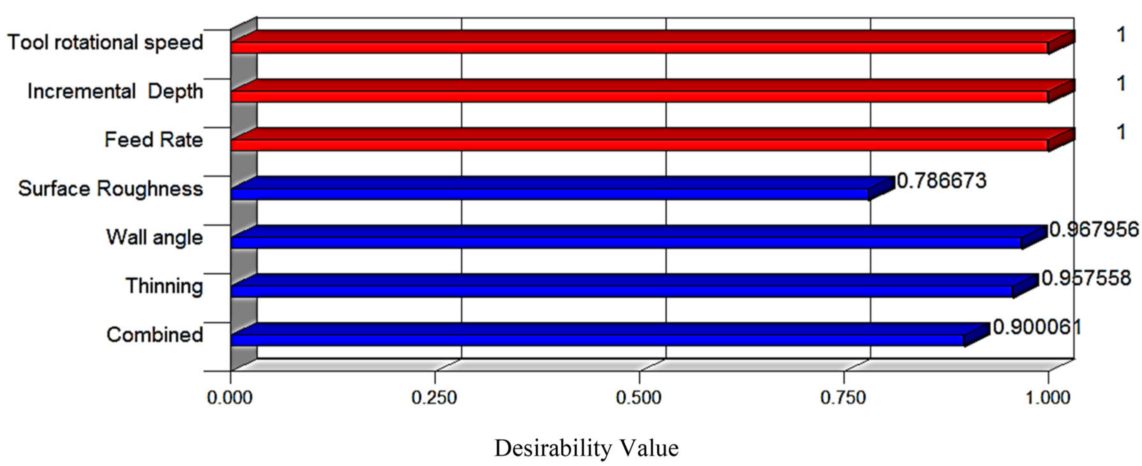


**Fig. 12** Histogram of the best solution

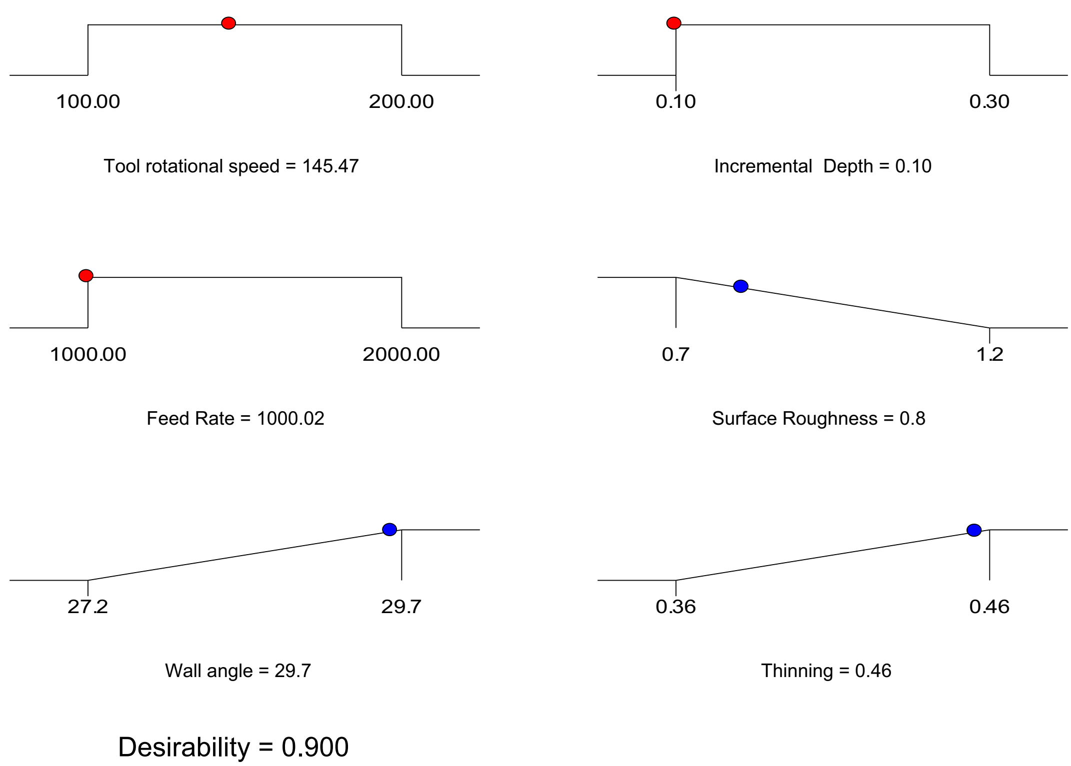


**Fig. 13** Ramp plot for optimal responses

d. Numerical optimization has been performed, and running confirmatory experiment with optimal parameters results in 2.5%, 4.5%, and 0.2% deviation from the actual desired values.

## References


1. Jong-Jin P, and Yung-Ho Kim. *J Mater Process Technol* **140** (2003) 447
2. Kopac J, Kampus Z, *J Mater Process Technol* **162–163** (2005) 622.
3. Kim Y H, Park J J, (2002) *J Mater Process Technol* **130–131** (2002) 42.
4. Cerro E M, Arana J, Rivero A, Rodrıguez P P, *J Mater Process Technol* **177** (2006) 404.
5. TalebAraghi B, Manco G L, Bambach M, Hirt G, *CIRP Ann Manuf Technol* **58** (2009) 225.
6. Capece Minutolo F, Durante M, Formisano A, and Langella A, *J Mater Process Technol* **194** (2007) 145.
7. Yao Z, Li Y, Yang M, Yuan Q, and Shi P, *Adv Mech Eng* **9** (2017) 1.
8. Jadhav S, *Basic investigations of the Incremental Sheet Metal Forming Process*, Doctorate thesis, University of Dortmund, Germany (2015).
9. Bhattacharya A, Maneesh K, Venkata Reddy N, Cao J, *J Manuf Sci Eng* **133** (2011) 0610201.
10. Hussaina G, Gaoa L, Hayat N, Zirana X, *J Mater Process Technol* **209** (2009) 4237.